npj | biofilms and microbiomes

Article

Published in partnership with Nanyang Technological University

https://doi.org/10.1038/s41522-024-00564-y

Akkermansia muciniphila in the small intestine improves liver fibrosis in a murine liver cirrhosis model

Noriaki Oguri[1], Jun Miyoshi[1] ✉, Yuu Nishinarita[1], Haruka Wada[1], Nobuki Nemoto[1], Noritaka Hibi[1], Naohiro Kawamura[1], Sawako Miyoshi[2], Sonny T. M. Lee[3], Minoru Matsuura[1], Takako Osaki[4] & Tadakazu Hisamatsu[1] ✉

Recent evidence indicates that liver cirrhosis (LC) is a reversible condition, but there is no established intervention against liver fibrosis. Although the gut microbiota is considered involved in the pathogenesis of LC, the underlying mechanisms remain unclear. Although the antibiotic, rifaximin (RFX), is effective for hepatic encephalopathy (HE) with LC, the impact of RFX on intestinal bacteria is unknown. We investigated the bacterial compositions along the GI tract under RFX treatment using a murine LC model. RFX improved liver fibrosis and hyperammonemia and altered the bacterial composition in the small intestine. The efficacy of RFX was associated with increases in specific bacterial genera, including *Akkermansia*. Administration of a commensal strain of *Akkermansia muciniphila* improved liver fibrosis and hyperammonemia with changing bacterial composition in the small intestine. This study proposed a new concept "small intestine-liver axis" in the pathophysiology of LC and oral *A. muciniphila* administration is a promising microbial intervention.

Chronic liver diseases result in liver fibrosis, which leads to liver cirrhosis (LC). LC is a crucial health issue throughout the world, although the prevalence of its etiologies (e.g., viral hepatitis, alcohol-associated liver disease, and nonalcoholic fatty liver disease) varies across times and geographic areas[1]. An epidemiological report showed that 2.4% of global deaths were associated with LC in 2019[2]. Recent evidence indicates that liver fibrosis is slowly reversible in patients with LC when the cause of chronic hepatitis is treated[3–6]. This finding suggests that an intervention that promotes an improvement in liver fibrosis should ensure a better prognosis in patients with LC. In the management of LC, it is also crucial to control various clinical complications, including hepatic encephalopathy (HE). HE is caused by liver insufficiency or portosystemic shunt, and manifests as a wide spectrum of neuropsychiatric symptoms, ranging from subclinical changes to coma[7–9]. HE reduces the patient's quality of life (QOL) and adversely affects the course of LC[10–12]. Even asymptomatic, minimal, or covert HE increases various risks in daily life, such as falls, traumatic injuries, and traffic accidents[13–15]. The gut microbiota is thought to be involved in the pathogenesis of LC and HE. Several studies have reported that the microbial components of the gut and their products (e.g., endotoxins, peptidoglycan, and bacterial DNA) play a role in the development of LC[16,17]. It has been reported that the composition of the gut microbiota in patients with LC differs from that in healthy people[18–20]. Although the pathophysiology of HE remains to be established, gut-derived neurotoxins, including ammonia, gamma-amino butyric acid (GABA), aromatic amino acids, and inflammatory cytokines, produced by the gut microbiota are considered to contribute to the development and deterioration of HE[21,22]. In clinical practice, a combination of nonabsorbable synthetic disaccharides and antibiotics has been used for many years as an effective therapy for HE[23]. Today, rifaximin (RFX), a nonabsorbable broad-spectrum antibiotic, is orally administered as an HE therapy[24]. RFX inhibits bacterial RNA synthesis by binding to the β-subunit of the bacterial DNA-dependent RNA polymerase[25]. Although the efficacy of RFX for HE is established, the underlying mechanism remains unclear. Several studies have reported that RFX reduces the expression of bacterial virulence factors and renders intestinal cells resistant to bacterial colonization and internalization[26,27]. Although it seems reasonable to expect that RFX exerts its effect by reducing the bacterial load and changing the microbial composition in the gut, various human and animal studies have reported that the fecal microbiome does not change after the administration of RFX[20,23,28]. However, we should note that those studies analyzed fecal samples as representative of the gut microbiome. Because the gut microbiota varies among the anatomical sites in the gastrointestinal (GI) tract[29], such fecal analyses are limited in their assessment of the impact of RFX on the

[1]Department of Gastroenterology and Hepatology, Kyorin University School of Medicine, Mitaka, Tokyo, Japan. [2]Department of Preventive Medicine, Kyorin University School of Medicine, Mitaka, Tokyo, Japan. [3]Division of Biology, Kansas State University, Manhattan, KS, USA. [4]Department of Infectious Diseases, Kyorin University School of Medicine, Mitaka, Tokyo, Japan. ✉e-mail: jmiyoshi@ks.kyorin-u.ac.jp; thisamatsu@ks.kyorin-u.ac.jp

overall gut microbiota. We hypothesized that the effects of RFX differ across different sites in the GI tract and that analyzing the effects of RFX on the gut microbiota along the GI tract should not only clarify the mechanism of RFX but also extend our understanding of the role of the gut microbiota in the pathophysiology of LC and HE. In this study, we used a murine model of LC to investigate the clinical efficacy of RFX and to investigate the effects of RFX on the gut microbiota at various anatomical sites along the GI tract of the model. A murine model could provide scientific merits while there are some limitations including differences in microbiome between host species and behaviors such as coprophagy. We identified a bacterial strain associated with the efficacy of RFX and examined the therapeutic potential of this strain for LC and HE.

Results

Administration of RFX improved liver fibrosis and hyperammonemia in a murine model of LC

A carbon tetrachloride (CCl_4)-induced mouse model of LC was used in this study. We injected CCl_4 into the peritoneum of specific-pathogen-free (SPF) mice three times a week for 6 weeks. The LC group showed severe fibrosis with nodule formation in the liver. The area of fibrosis was significantly larger in the LC group than in the control group (10.38 ± 0.75% vs 0.70 ± 0.25%, respectively; $p < 0.0001$; Fig. 1A). The blood ammonia (NH_3) concentration was significantly higher in the LC group (640.3 ± 16.9 μg/dL) than in the control group (501.5 ± 26.2 μg/dL; $p = 0.0014$; Fig. 1B). We next prepared three groups to assess the impact of RFX on the gut microbiota: (1) the LC-no treatment (NTx) group was administered oral phosphate-buffered saline (PBS; vehicle) for 4 weeks after the induction of LC; (2) the LC-RFX groups was orally administered RFX for 4 weeks after the induction of LC; and (3) the control-NTx group included healthy control mice without LC (intraperitoneally administered olive oil [vehicle] followed by the oral administration of PBS [vehicle]) (Fig. 1C). The area of fibrosis was significantly smaller in the LC-RFX group (4.709 ± 0.2048%) than in the LC-NTx group (6.74 ± 0.24%; $p = 0.0351$; Fig. 1D). The fibrotic area was larger in the LC group than in the other groups. These findings are consistent with the spontaneous improvement in liver fibrosis over time in the CCl_4-induced murine model of LC[30]. The blood NH_3 concentration was significantly lower in the LC-RFX group (567.2 ± 20.6 μg/dL) than in the LC-NTx group (680.3 ± 18.2 μg/dL; $p = 0.0053$; Fig. 1E). There was a positive correlation between the area of fibrosis and the blood NH_3 concentration (Fig. 1F). In the liver, the expression of the mouse transforming growth factor β gene (*Tgfb*) and acetyl-CoA carboxylase alpha gene (*Acca*), a fibrotic marker, was significantly lower in the LC-RFX group than in the LC-NTx group ($p = 0.0066$). The expression of mouse genes involved in bacterial recognition and inflammation, including Toll-like receptor 2 (*Tlr2*), *Tlr4*, and tumor necrosis factor (*Tnf*), was significantly lower in the LC-RFX group than in the LC-NTx group ($p = 0.0071$, $p = 0.0429$, and $p = 0.0370$, respectively; (Fig. 1G)). The portal endotoxin concentration was significantly lower in the LC-RFX group (0.1895 ± 0.0224 EU/mL) than in the LC-NTx group (0.2998 ± 0.0303 EU/mL; $p = 0.0440$; Fig. 1H). Taken together, these results suggest that RFX improves fibrosis and hyperammonemia in LC by reducing both bacteria-derived components that enter the host via the portal vein and inflammation in the liver.

Changes in bacterial composition induced by RFX in the small intestine are associated with clinical improvement

We examined the gut microbiota at multiple sites in the GI tract (jejunum, ileum, cecum, and colon) and in the stools of our murine model. The bacterial loads were assessed with a quantitative PCR (qPCR) analysis of the bacterial *tuf* gene. There were no significant differences in the bacterial loads in the LC-RFX group and the LC-NTx groups in either sex (Fig. 2A and Supplementary Fig. 1A). 16S rRNA gene amplicon sequencing demonstrated that Shannon diversity index increased in the ileal and cecal contents in male animals (Fig. 2B) and in the jejunal and ileal contents in female animals (Supplementary Fig. 1B) in the LC-RFX group compared with the findings in the LC-NTx group (male ileum $p = 0.0292$ and cecum $p = 0.0173$; female jejunum $p = 0.0053$ and ileum $p = 0.0305$). A principal coordinate analysis (PCoA) plot of all samples based on weighted UniFrac distances is shown in Fig. 2C and Supplementary Fig. 1C. The sizes of the compositional changes at each GI site and in the stools were quantitatively compared between the LC-RFX and LC-NTx groups based on weighted UniFrac distances. The jejunal and ileal contents showed greater changes than the cecal or colonic contents in male animals (Fig. 2D) and the jejunal contents showed the greatest compositional change in female animals (Supplementary Fig. 1D). Overall, RFX affected the small-intestinal bacteriome more strongly than the cecal, colonic, or fecal bacteriome in both sexes of the murine model of LC. The relative abundances of bacteria at the phylum and genus levels in all samples are presented in Supplementary Fig. 2A–C. Multivariable association analyses of the clinical features of the model (liver fibrosis and blood NH_3 concentration) and the bacterial compositions at the genus level in the jejunum and ileum (adjusted for sex) were undertaken. The relative abundances of *Faecalibaculum*, *Akkermansia*, and *Muribaculaceae* correlated negatively with liver fibrosis in both the jejunum and ileum, whereas *Streptococcus* and *Clostridia_UCG.014* correlated positively with liver fibrosis in the both jejunum and ileum (Fig. 2E). These findings suggest that the increases in the genera *Faecalibaculum*, *Akkermansia*, and *Muribaculaceae* in the small intestine were associated with the improvement of liver fibrosis and that this may be one of mechanisms by which hyperammonemia is improved. On the host side, in the small-intestinal mucosa, the expression of claudin 3 (*Cldn3*), *Cldn4*, and *Cldn15* was significantly higher in the LC-RFX group than in the LC-NTx group. The expression of antimicrobial peptides, *Tlr2*, and *Tlr4* was lower in the LC-RFX group compared with the LC-NTx group (Supplementary Fig. 3). These changes were not apparent in the colonic mucosa (Supplementary Fig. 4). Therefore, gene expression in the host mucosa may be affected by changes in the intestinal microbiome.

Administration of *A. muciniphila* improved liver fibrosis and hyperammonemia

Akkermansia was the only bacterial genus detected in the phylum Verrucomicrobiota in our 16S rRNA gene amplicon sequencing analysis and this genus showed decreased abundance in the animals with CCl4-induced LC compared with the controls (Supplementary Fig. 2B). Shotgun metagenomic sequencing of the jejunal and ileal contents showed that within the genus *Akkermansia*, only *A. muciniphila* SGB9226 was detected in our samples. *A. muciniphila* SGB9226 is the same species-level genome bin (SGB) as *A. muciniphila* ATCC BAA-835 (AKK), a genomically defined strain[31,32]. Therefore, we investigated the clinical efficacy of supplementation of the murine CCl_4-induced model of LC with AKK: (1) the LC-AKK group was orally administered AKK (1×10^9 CFU/day in a mouse) for 4 weeks after the induction of LC; and (2) the LC-NTx2 group was orally administered PBS with 10% glycerol (vehicle) for 4 weeks after the induction of LC (Fig. 3A). The area of fibrosis in the liver was significantly smaller in the LC-AKK group (5.18 ± 0.13%) than in the LC-NTx2 group (5.86 ± 0.15%; $p = 0.0012$; Fig. 3B). The blood NH_3 concentration was significantly lower in the LC-AKK group (719.5 ± 19.2 μg/dL) than in the LC-NTx2 group (839.3 ± 33.0 μg/dL; $p = 0.0006$; Fig. 3C). The expression of *Tgfb*, *Acca*, and collagen type I-alpha 1 (*Col1a1*) was significantly lower in the LC-AKK group than in the LC-NTx2 group ($p = 0.0004$). The expression of *Tlr2* and *Tnfa* was significantly lower in the LC-AKK group than in the LC-NTx2 group ($p = 0.0263$ and $p = 0.0211$, respectively; Fig. 3D). The portal endotoxin concentration was significantly lower in the LC-AKK group (0.0992 ± 0.0171 EU/mL) than in the LC-NTx2 group (0.1911 ± 0.0356 EU/mL; $p = 0.0343$; Fig. 3E). These findings are consistent with those observed after the RFX treatment (Fig. 1). There were no apparent adverse events due to AKK supplementation, although the animals in the LC-AKK group tended to show less bodyweight gain than those in the control group, as previously reported[33,34] (Supplementary Fig. 5). Our results demonstrate the potential utility of AKK as a probiotic to improve liver fibrosis and hyperammonemia, and suggest that the underlying mechanisms involved in the clinical efficacy of AKK supplementation are similar to those involved in treatment with RFX.

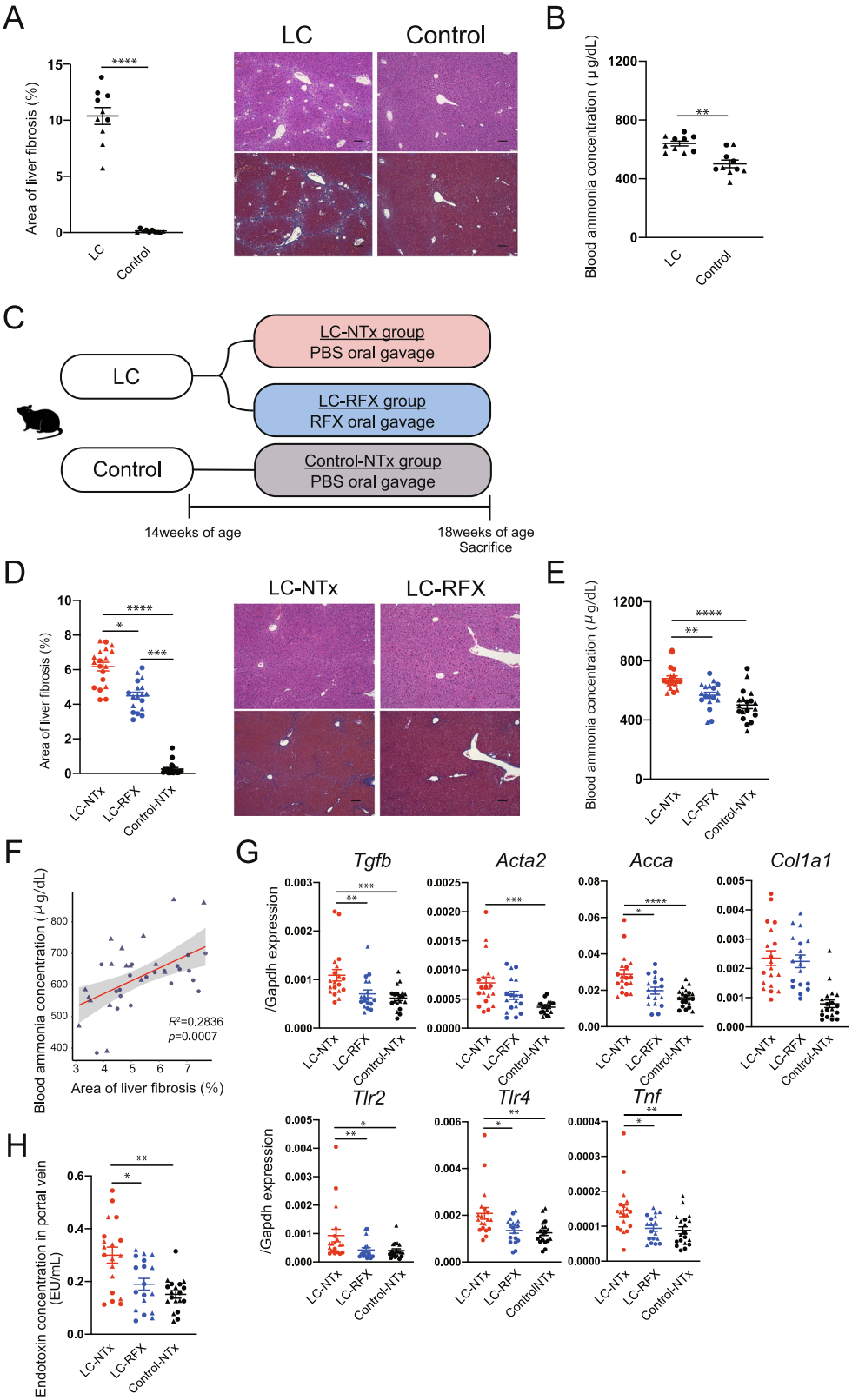

Fig. 1 | Rifaximin improved liver fibrosis and hyperammonemia in a murine model of liver cirrhosis. **A** Quantification of the area of liver fibrosis in the liver cirrhosis (LC) group ($n = 10$) and control group ($n = 10$). Representative microscopic images of liver tissues stained with hematoxylin and eosin and Azan from each group are shown. Scale bars: 100 μm. **B** Blood ammonia concentrations in the LC and control groups. **C** Study design to assess the impact of rifaximin (RFX) on the gut microbiota. **D** Quantification of the area of liver fibrosis in the LC-no treatment (NTx) group ($n = 19$), the LC-RFX group ($n = 18$), and the control-NTx group ($n = 19$). Representative microscopic images of liver tissues from the LC-NTx and LC-RFX groups are shown. Scale bars: 100 μm. **E** Blood ammonia concentrations in the LC-NTx, LC-RFX, and control-NTx groups. **F** Correlation analysis of the area of liver fibrosis and blood ammonia concentration in the LC-NTx, LC-RFX, and control-NTx groups. **G** mRNA expression in the liver tissues of the LC-NTx, LC-RFX, and control-NTx groups. **H** Endotoxin concentrations in the portal veins in the LC-NTx, LC-RFX, and control-NTx groups. Data are means ± standard errors of the means (circle: male; triangle: female). $^{*}p < 0.05$, $^{**}p < 0.01$, $^{***}p < 0.001$, $^{****}p < 0.0001$, Mann–Whitney U test for two groups, Kruskal–Wallis test and Dunn's test for three groups. Correlation analysis was performed with Spearman's rank correlation coefficient.

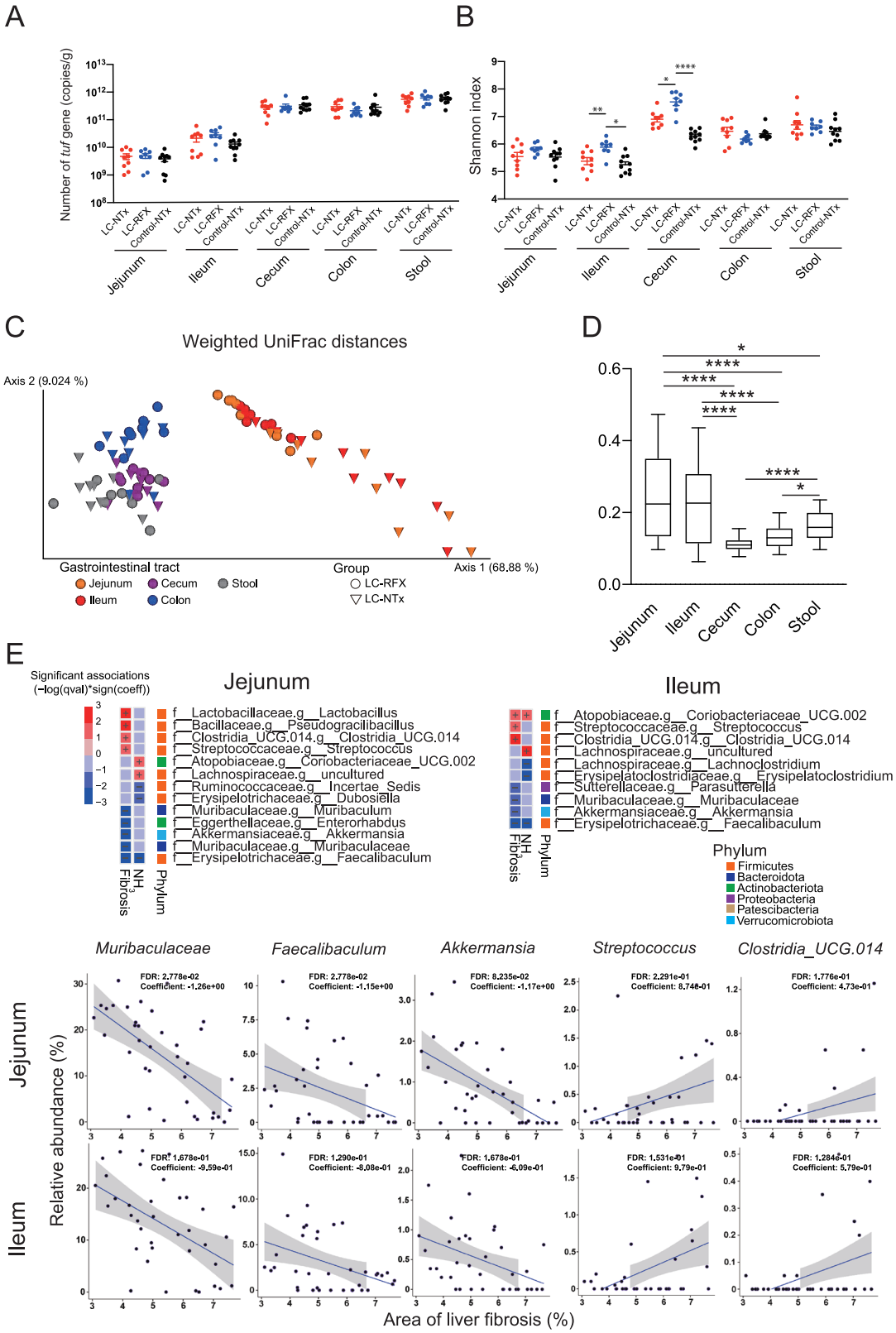

Fig. 2 | Analysis of gut microbiota at multiple sites in the gastrointestinal tract and stools. A Bacterial load evaluated with qPCR of *tuf* gene in male animals of the liver cirrhosis (LC)-no treatment (NTx) group ($n = 9$), the LC-rifaximin (RFX) group ($n = 8$), and the control-NTx group ($n = 10$). **B** Shannon diversity indices for the gastrointestinal (GI) sites and stools of male animals in the LC-NTx group, the LC-RFX group, and the control-NTx group. **C** Principal coordinates analysis (PCoA) plot based on weighted UniFrac distances of bacterial compositions in male animals in the LC-NTx group and LC-RFX group. **D** Differences in weighted UniFrac distances at each GI site and in stools of the LC-NTx group and the LC-RFX group. **E** Multivariate association analysis of the clinical features (area of liver fibrosis and blood ammonia concentration) and bacterial compositions at the genus level in the jejunum and ileum using samples from both sexes with adjustment for sex ($n = 19$ in the LC-NTx group and $n = 18$ in the LC-RFX group). Data on bacterial load, Shannon index, PCoA plot, and weighted UniFrac distances in female animals are shown in Supplementary Fig. 2. Data are means ± standard errors of the means. $^{*}p < 0.05$, $^{**}p < 0.01$, $^{***}p < 0.001$, $^{****}p < 0.0001$, Kruskal–Wallis test and Dunn's test.

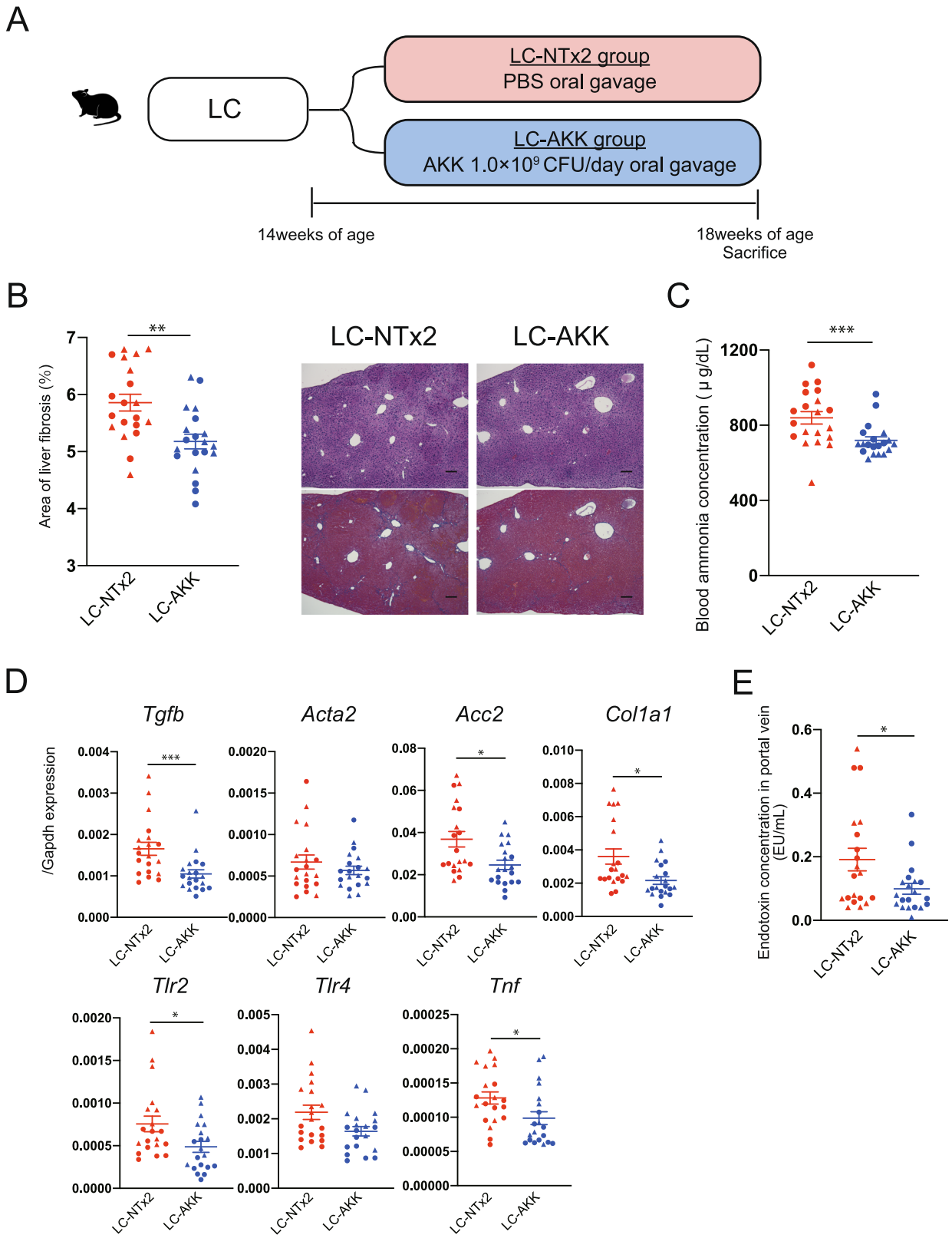

Fig. 3 | *Akkermansia muciniphila* improved liver fibrosis and hyperammonemia in a murine model of liver cirrhosis. A Study design to assess the effects of *Akkermansia muciniphila*. **B** Quantification of area of liver fibrosis in the liver cirrhosis (LC)-no treatment (NTx)2 group ($n = 20$) and the LC-*Akkermansia* (AKK) group ($n = 20$). Representative microscopic images of liver tissues stained with hematoxylin and eosin and Azan are shown. **C** Blood ammonia concentrations in the LC-NTx2 and LC-AKK groups. **D** mRNA expression in the liver tissues of the LC-NTx2 and LC-AKK groups. **E** Endotoxin concentrations in the portal veins of the LC-NTx2 and LC-AKK groups. Data are means ± standard errors of the means (circle: male; triangle: female). $^{*}p < 0.05$, $^{**}p < 0.01$, $^{***}p < 0.001$, Mann–Whitney *U* test.

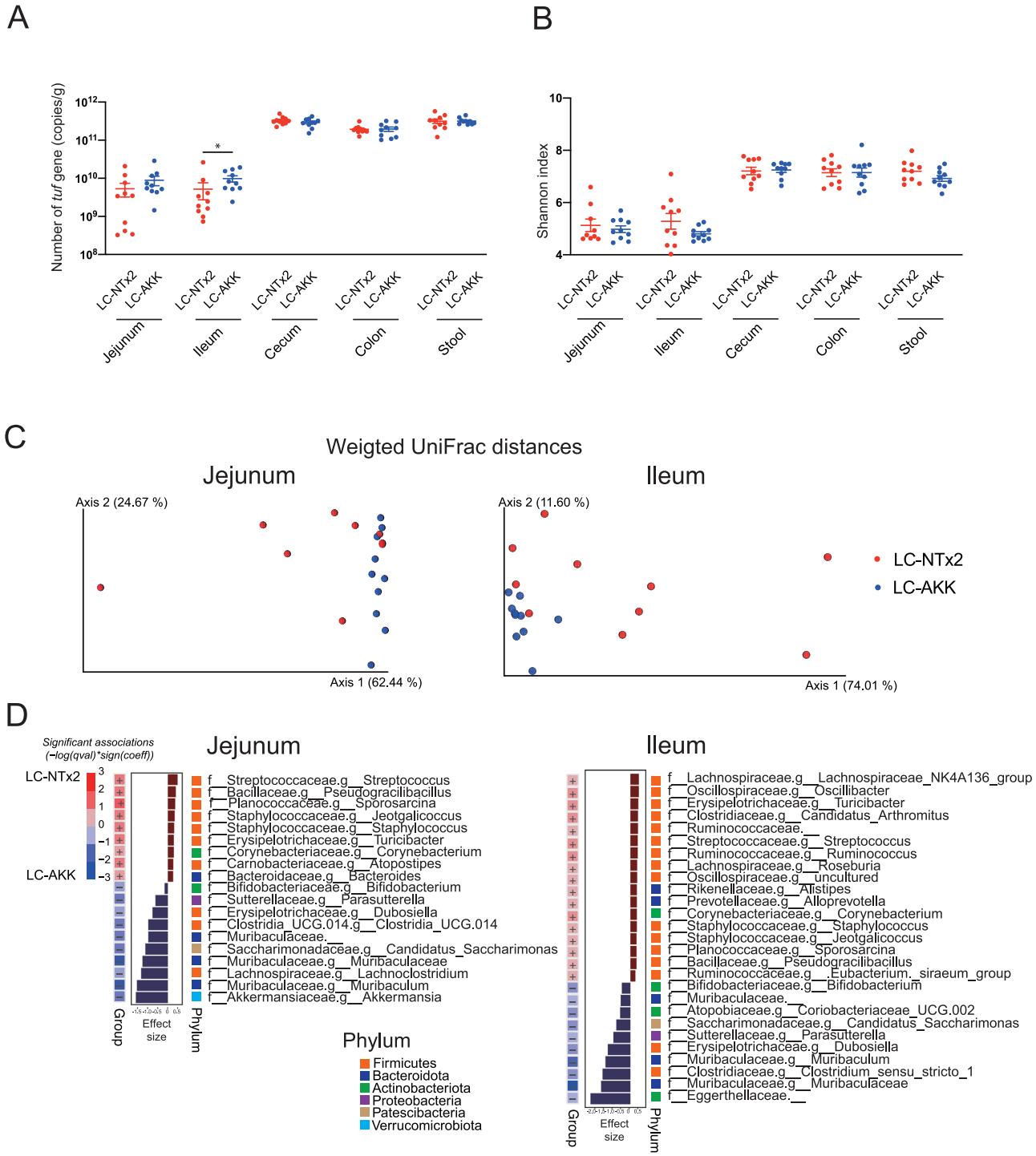

Fig. 4 | *Akkermansia muciniphila* induced compositional changes in the small-intestinal microbiota. A Bacterial load evaluated with qPCR of *tuf* gene in male animals in the liver cirrhosis (LC)-no treatment (NTx)2 group ($n = 10$) and the LC-*Akkermansia* (AKK) group ($n = 10$). **B** Shannon diversity index in male animals of the LC-NTx2 and LC-AKK groups. **C** Principal coordinates analysis (PCoA) plots based on weighted UniFrac distances of bacterial composition in the jejunum and ileum in male animals in the LC-NTx2 and LC-AKK groups. **D** Multivariate association analysis between two groups (the LC-NTx2 and LC-AKK groups) and bacterial composition at the genus level in the jejunum and ileum using samples from both sexes, with adjustment for sex ($n = 20$ in both the LC-NTx2 and LC-AKK groups). Data on bacterial load, Shannon index, and PCoA plots in female animals are shown in Supplementary Fig. 7. Data are means ± standard errors of the means. $^*p < 0.05$, Mann–Whitney *U* test. Bacterial composition was compared with permutational analysis of variance.

Administration of *A. muciniphila* affects the bacterial composition in the small intestine

The relative abundance of the genus *Akkermansia* in the cecum was significantly higher in the LC-AKK group than in the LC-NTx2 group, demonstrating that orally administered AKK reached the lower GI tract (Supplementary Fig. 6). We examined the gut microbiota at multiple sites in the GI tract and in the stools. The bacterial load did not change overall, except for an increase in the ileum in the male animals in the LC-AKK group (Fig. 4A and Supplementary Fig. 7A). 16S rRNA gene amplicon sequencing demonstrated that Shannon diversity index did not differ between the LC-AKK and LC-NTx2 groups in the male animals (Fig. 4B), and the female animals showed the same tendency (Supplementary Fig. 7B). In the PCoA

plots based on weighted UniFrac distances, the bacterial compositions in the small intestines of the LC-AKK and LC-NTx2 groups clustered separately (male jejunum $p = 0.001$ and ileum $p = 0.003$; female jejunum $p = 0.002$ and ileum $p = 0.001$; Fig. 4C and Supplementary Fig. 7C). The relative abundances of bacteria at the phylum and genus levels in all the samples are presented in Supplementary Fig. 8A–C. An association analysis at the genus level, adjusted for sex, demonstrated that the relative abundance of *Akkermansia* and *Muribaculaceae* in the jejunum was higher in the LC-AKK group than in the control group and that the relative abundance of *Muribaculaceae* in the ileum was higher in the LC-AKK group than in the control group, whereas the relative abundances of *Streptococcus* in the jejunum and ileum were lower in the LC-AKK group than in the LC-NTx2 group (Fig. 4D). These findings are consistent with our finding that the increase in *Muribaculaceae* and the reduction in *Streptococcus* in the small intestine was associated with an improvement in liver fibrosis (Fig. 2E). In the host, the changes in gene expression in the ileal mucosa after the administration of AKK were similar to those observed after RFX treatment. The expression of *Cldn2*, *Cldn3*, and occluding (*Ocln*) was significantly higher in the small intestinal mucosa of the LC-AKK group than in that of the control group. The expression of regenerating islet-derived 3 gamma (*Reg3g*) and *Tlr4* was significantly lower in the ileal mucosa and jejunal mucosa, respectively, of the LC-AKK group than in those of the LC-NTx2 group (Supplementary Fig. 9). The AKK-induced changes in gene expression in the colonic mucosa showed similar tendencies but were weaker than those in the ileal mucosa, as we observed in the animals treated with RFX (Supplementary Fig. 10). These findings imply that the administration of AKK affects the interactions between the small intestinal microbiome and the host intestinal mucosa.

Discussion

In the present study, we have demonstrated that changes in the small-intestinal bacterial composition, including an increase in *Akkermansia*, are associated with an improvement in liver fibrosis and hyperammonemia and that the administration of a strain of *A. muciniphila* improved liver fibrosis and hyperammonemia in a murine model of LC. This murine model showed improvement in fibrosis over time after the cessation of CCl_4 treatment, and the administration of *A. muciniphila* advanced this process. Although the progression of liver fibrosis to LC has been considered irreversible, recent reports have demonstrated that the successful treatment of chronic liver disease can improve fibrosis, regardless of the pathoetiology of the liver disease[3–6,35]. Our murine model also shows an improvement in liver fibrosis over time. Although we need to consider the limitations of the animal model and differences in pathophysiology between murine and human LC, our findings could provide insights relevant to human clinical practice. In this respect, using a murine model of LC provides scientific merit, although the differences in the microbiota between host species need to be considered. This improvement in liver fibrosis should contribute to better clinical outcomes and longer survival by reducing critical morbidity, including the risk of liver failure and hepatocellular carcinoma[36]. However, a therapeutic intervention for liver fibrosis remains a crucial unmet need. Our study has clinical significance in proposing a new strategy for improving liver fibrosis after the treatment of the associated chronic liver disease (i.e., removing the cause of liver damage). Furthermore, because the oral administration of *A. muciniphila* improved hyperammonemia, our findings suggest a microbial intervention for HE, including minimal or covert HE, to improve the patient's QOL and prognosis, and the associated socio-economic burden. Meanwhile, it should be noted that ammonia is not the single causative agent of HE, and thoughtful extrapolation of the results is needed for human HE.

In this study, correlation analysis identified three genera that are potentially beneficial against liver fibrosis: *Faecalibaculum*, *Akkermansia*, and *Muribaculaceae*. Based on this finding, we speculated the possibility that each of these genera could have beneficial impacts and also that multiple bacteria collectively may be more effective than a single strain. However, there were various practical hurdles to conducting experiments using these genera. First, given that it is difficult to culture *Muribaculaceae*[37], we considered that using this genus for clinical intervention may not be practical. In addition, our metagenome shotgun sequencing demonstrated that the genus *Muribaculaceae* included multiple species and we could not identify a single strain for isolation and culture to investigate clinical efficacy. Several recent studies reported that *Faecalibaculum rodentium*, a representative microbe of the genus *Faecalibaculum*, has beneficial effects on the host. Metagenome shotgun sequencing only identified *F. rodentium* within the genus *Faecalibaculum*[38,39] in our samples. Therefore, we tried to culture the representative strain of this microbe. However, we could not obtain sufficient bacteria for the oral administration experiment. Also, this microbe is not a commensal in humans. We considered that this microbe is also not practical as a potential probiotic for clinical application. We, therefore, decided on *A. muciniphila* as the most suitable genus for clinical application because it can be identified at the strain level and is easy to culture under anaerobic conditions. It is also an advantage for the clinical application of *A. muciniphila* that it is a commensal microbe in humans[40,41]. Therefore, we focused on *A. muciniphila* in this study.

A. muciniphila is a mucin-degrading, Gram-negative, nonmotile, anaerobic bacterium that lives in the mucus layer and epithelial crypts of the small intestine in humans and other animals[42]. A low abundance of *A. muciniphila* is reportedly associated with several diseases, including type 2 diabetes mellitus, obesity, inflammatory bowel disease, and colon cancer[40,43–45]. Several studies have shown that supplementation with the microbe exerts beneficial effects against host metabolic and immune dysfunction in animal models[33,34,46]. Our finding that animals administered *A. muciniphila* showed less weight gain is consistent with these reports. Some reports suggested that oral administration of AKK suppresses the progression of liver fibrosis or liver injury in the murine models using high-fat diet/CCl_4 or alcohol[47–49]. In contrast, the present study is the first to demonstrate the beneficial effects of *A. muciniphila* on the improvement of liver fibrosis and hyperammonemia.

Bacterial compounds (e.g., endotoxins), which enter the host via the portal vein, are considered to play roles in the progression of liver fibrosis. These compounds act as pathogen-associated molecular patterns, binding to pattern-recognition receptors, such as toll-like receptors, which activate the signaling pathways of various inflammatory cytokines, which ultimately induce liver fibrosis[50]. Gut dysbiosis arising from liver fibrosis also increases intestinal permeability, increasing the levels of endotoxin in the plasma[17]. These vicious cycles contribute to the progression of liver fibrosis and hyperammonemia. Although the colon has been considered a major site of these interactions[51], this study has shown that the small-intestinal microbiota plays a crucial role in the pathogenesis of liver fibrosis and hyperammonemia. Our findings suggest the novel concept of a "small intestine–liver axis" involved in the pathophysiology of LC and HE.

The changes in the bacterial composition in the small intestine induced by the administration of *A. muciniphila* could exert its clinical effect by changing the microbial metabolites and compounds in the gut. Beneficial changes in the intestinal barrier function could be another mechanism underlying the clinical effect of *A. muciniphila* on liver fibrosis and hyperammonemia. Plovier et al. reported that *A. muciniphila* enhances the integrity of the intestinal barrier and reduces the flow of endotoxin from the gut microbiota to the bloodstream[34]. The small-intestinal bacterial transcriptomes determined in this study are consistent with their findings. While the impact of *A. muciniphila* on the expression of *Reg3g* remains controversial[34,44,52], the present study demonstrated a decrease in the expression level of *Reg3g* in the ileum of animals following AKK administration. Given that *Reg3g* expression increased in our murine LC model, LC causes dysbiosis, and various bacteria could impact *Reg3g* expression[53,54], there is a possibility that administration of AKK corrected the aberrant expression of *Reg3g* under LC-related dysbiosis. Because the composition and physiological significance of the gut microbiota vary between anatomical sites[29], it is challenging to investigate the small-intestinal microbiota in humans. In this respect, using a murine model of LC provides our study with scientific merit. However, even with an animal model, there are limitations

to tracking changes in the small-intestinal microbiota over time in living individual animals during a microbial intervention. Another limitation of this study is that we cannot exclude the possibility that the *A. muciniphila* administered interacted with the host in the colon in addition to the small intestine because at least some of the administered bacterium may have traversed the intestinal tract and reached the colon. However, our findings regarding the RFX treatment support the notion that *A. muciniphila* in the small intestine, but not in the colon, is a key to improving fibrosis and hyperammonemia. Furthermore, given that mice are coprophagous, another limitation of this animal study is that it excludes the potential impact of coprophagy on the intestinal microbiome, including the small intestine[55], and on the beneficial clinical effects. Further studies are needed to address this challenge.

In conclusion, the oral administration of *A. muciniphila* exerted a clinical effect against liver fibrosis and hyperammonemia in a murine model of LC. While there are limitations in the murine LC model to recapitulate human pathophysiology, our study provides new insights into the role of the "small intestine–liver axis" in LC and HE. Because *A. muciniphila* is commensal in humans, this microbe could have the potential to be a novel therapeutic strategy for human liver fibrosis and HE.

Methods

Animals

Specific-pathogen-free (SPF) wild-type C57Bl/6J mice (4 weeks of age) were purchased from CLEA Japan (Tokyo, Japan). The mice were maintained and treated under SPF conditions on a 12:12-h light:dark cycle. The mice were fed gamma-sterilized CLEA Rodent Diet CE-2 (CLEA Japan) and supplied with drinking water *ad libitum*. The bedding transfer protocol[56] was performed twice a week for 4 weeks before the experiments were commenced to normalize the gut microbiota. All mice were euthanized at the end of the study with carbon dioxide inhalation and cervical dislocation. The experiments were reviewed and approved by the Experimental Animal Ethics Committee at Kyorin University (Tokyo, Japan; approval numbers 242 and 262). All animal experiments were conducted according to the Japanese guidelines for experimental animal welfare and study protocols. The authors complied with the ARRIVE guidelines for reporting.

Carbon tetrachloride intraperitoneal injection

Carbon tetrachloride (CCl_4) was obtained from FUJIFILM Wako Pure Chemical Corporation (Tokyo, Japan). CCl_4 (0.5 mL/kg of mouse bodyweight) was dissolved in olive oil (Wako Pure Chemical Co.) and made up to a total volume of 100 µL with the oil. CCl_4/olive oil solution (100 µL) was administered to each mouse by intraperitoneal injection with a 26G needle three times a week for 6 weeks (from 8 to 14 weeks of age).

Rifaximin administration

RFX was purchased from Sigma-Aldrich (St. Louis, MO, USA) and suspended in PBS with 0.5% Tween 80 (CLEA Japan). The dose of RFX was calculated based on the normalization method, using the body surface area[57,58]. An RFX dose of 1200 mg/day is the insurance-approved dose for a 60 kg person suffering HE in Japan, and the equivalent dose for a mouse was calculated to be 246 mg/kg/day. The mice were orally administered 200 µL of RFX solution every day for 4 weeks (from 14 to 18 weeks of age).

Akkermansia muciniphila culture and administration

A. muciniphila ATCC BAA-835 (AKK) was purchased from RIKEN BioResource Center (Ibaraki, Japan). The microbe was cultured anaerobically (CO_2: 10%, H_2: 10%, N_2: base) in brain–heart infusion broth with 0.5% type II mucin from the porcine stomach (Sigma-Aldrich) at 37 °C. The colony-forming units (CFU) per milliliter were determined on Anaero Columbia agar with rabbit blood (Nippon Becton Dickinson Co., Ltd, Tokyo, Japan) under anaerobic conditions. The cultured AKK was centrifuged and washed using PBS. The AKK stock (1×10^{10} CFU/mL) was prepared in anaerobic PBS and 20% glycerol (Nacalai Tesque, Inc., Kyoto, Japan) and stored at −80 °C. The AKK stock was diluted with anaerobic PBS to 5×10^9 CFU/mL under anaerobic conditions just before its oral administration to mice. The mice were orally administered 200 µL (1×10^9 CFU) of AKK solution every day for 4 weeks (from 14 to 18 weeks of age).

Measurement of blood ammonia concentrations

Blood samples were collected by cardiac puncture with a 21G needle. The blood ammonia concentration was immediately measured with the PocketChem BA PA-4140 (Arkray, Inc., Kyoto, Japan), according to the manufacturer's protocol.

Measurement of endotoxin concentrations in portal vein

Blood samples from the portal vein were collected with a 27G needle. The serum samples were obtained by centrifuging the whole blood at 10,000 × *g* for 10 min and were stored at −80 °C. The Hycult Biotech Limulus Amebocyte Lysate Chromogenic Endpoint Assay (Hycult Biotech, Uden, The Netherlands) was used to measure the endotoxin concentrations, according to the manufacturer's protocol.

Histological analysis

Liver tissues were fixed in 10% formalin solution and embedded in paraffin. AZAN staining was used to assess the area of fibrosis under microscopy. The percentage area of the liver tissue affected by fibrosis was quantified with the Hybrid Cell Count method with the BZ-X Analyzer software (Keyence, Osaka, Japan).

DNA extraction and 16S rRNA gene amplicon sequencing

Gastrointestinal tract contents from the jejunum, ileum, cecum, and colon, and from feces were collected and frozen at −80 °C. DNA was extracted from each intestinal content sample, as described previously[59]. Following the amplification of the 16S rRNA gene V4 region, the amplicons were sequenced on the MiSeq platform (Illumina, San Diego, CA, USA). The sequences were processed with Quantitative Insights in the Microbiome Ecology (QIIME2) pipeline[60]. The sequences were denoised and filtered with DADA2[61]. The sampling depth was set at 2000 based on the rarefaction curves for Shannon diversity index (Supplementary Fig. 11). The taxonomy of amplicon sequence variants was assigned with the Silva 138 database (https://docs.qiime2.org/2023.9/data-resources/). The diversity of the bacterial communities was investigated with QIIME2. Alpha diversity was evaluated with the Shannon diversity index. Beta-diversity was assessed with UniFrac distances and visualized with a principal coordinate analysis (PCoA).

Shotgun metagenomic sequencing analysis

Libraries were prepared with an Illumina DNA Prep (M) Tagmentation Library Preparation Kit (Illumina), according to the manufacturer's protocol, and 150-base pair-end reads were sequenced with the NextSeq 2000 Sequencing System (Illumina). The pair-end reads were merged with BBmerge[62]. Low-quality bases, low-quality reads, and adapters in the merged metagenomic reads were removed with Trimmomatic[63] and Tandem Repeats Finder[64]. Decontamination of the host genome was performed with KneadData using the mouse_C57BL_6NJ_Bowtie2_v0.1 database (http://huttenhower.sph.harvard.edu/kneadData_databases/). Taxonomic profiles at the species and species-level genome bins were obtained with MetaPhlAn4[65].

Bacterial counts in each intestinal and stool sample

The bacterial load in each intestinal content and stool sample was quantified with the Bacteria (*tuf* gene) Quantitative PCR Kit (Takara Bio Inc., Shiga, Japan), according to the manufacturer's protocol. The DNA samples used for 16S rRNA gene amplicon sequencing were also used for the quantitative PCR (qPCR) analysis of the *tuf* gene.

Reverse transcription–qPCR

RNA was extracted from liver tissues and each sample of intestinal mucosa with TRIzol Reagent (Thermo Fisher Scientific, Waltham, MA, USA),

according to the manufacturer's protocol. First-strand cDNA was synthesized with the High-Capacity cDNA Reverse Transcription Kit (Thermo Fisher Scientific), and qPCR was performed with PowerUp™ SYBR™ Green Master Mix for qPCR (Thermo Fisher Scientific) with QuantStudio™ 5 Real-Time PCR System (Thermo Fisher Scientific), according to the manufacturers' protocols. For each reverse transcription reaction, 100 ng of RNA was used. Primers were designed based on PrimerBank (https://pga.mgh.harvard.edu/primerbank/). The primers used for qPCR are listed in Supplementary Table 1.

Statistical analyses

All statistical analyses were performed with GraphPad Prism version 8.4.3 and R (version 4.1.3) (https://www.R-project.org/). The Mann–Whitney *U* test was used to compare values between two groups and the Kruskal–Wallis test and Dunn's test were used to compare values among three or more groups. Spearman's rank correlation coefficient was used to examine the correlation between the blood ammonia concentration and the area of liver fibrosis. Bacterial β-diversity was compared with permutational analysis of variance. The correlations between the relative abundances of genera and the ammonia concentration or area of liver fibrosis were assessed with the MaAsLin2 package[66] (https://github.com/biobakery/Maaslin2/). The criterion for statistical significance was set at a p-value < 0.05 or q-value < 0.05.

Data availability

The accession number for the microbial dataset and the mouse sample information reported in this paper is DRA: DRA017678 (https://www.ddbj.nig.ac.jp/dra/). The datasets generated and/or analyzed during the present study are available from the corresponding author on reasonable request.

Received: 6 March 2024; Accepted: 2 September 2024;
Published online: 16 September 2024

References

1. Huang, D. Q. et al. Global epidemiology of cirrhosis - aetiology, trends and predictions. *Nat. Rev. Gastroenterol. Hepatol.* **20**, 388–398 (2023).
2. The Global Health Observatory. Global health estimates: leading causes of death. WHO https://www.who.int/data/gho/data/themes/mortality-and-global-health-estimates/ghe-leading-causes-of-death (2023).
3. Marcellin, P. et al. Regression of cirrhosis during treatment with tenofovir disoproxil fumarate for chronic hepatitis B: a 5-year open-label follow-up study. *Lancet* **381**, 468–475 (2013).
4. Sun, Y. et al. New classification of liver biopsy assessment for fibrosis in chronic hepatitis B patients before and after treatment. *Hepatology* **65**, 1438–1450 (2017).
5. Pockros, P. J. et al. Histologic outcomes in hepatitis C-infected patients with varying degrees of virologic response to interferon-based treatments. *Hepatology* **52**, 1193–1200 (2010).
6. Mauro, E. et al. Portal pressure and liver stiffness measurements in the prediction of fibrosis regression after sustained virological response in recurrent hepatitis C. *Hepatology* **67**, 1683–1694 (2018).
7. Vilstrup, H. et al. Hepatic encephalopathy in chronic liver disease: 2014 Practice Guideline by the American Association for the Study of Liver Diseases and the European Association for the Study of the Liver. *Hepatology* **60**, 715–735 (2014).
8. Patidar, K. R. & Bajaj, J. S. Covert and overt hepatic encephalopathy: diagnosis and management. *Clin. Gastroenterol. Hepatol.* **13**, 2048–2061 (2015).
9. EASL. Clinical practice guidelines on nutrition in chronic liver disease. *J. Hepatol.* **70**, 172–193 (2019).
10. Hirode, G., Vittinghoff, E. & Wong, R. J. Increasing burden of hepatic encephalopathy among hospitalized adults: an analysis of the 2010-2014 national inpatient sample. *Dig. Dis. Sci.* **64**, 1448–1457 (2019).
11. Cordoba, J. et al. Characteristics, risk factors, and mortality of cirrhotic patients hospitalized for hepatic encephalopathy with and without acute-on-chronic liver failure (ACLF). *J. Hepatol.* **60**, 275–281 (2014).
12. Jepsen, P., Ott, P., Andersen, P. K., Sørensen, H. T. & Vilstrup, H. Clinical course of alcoholic liver cirrhosis: a Danish population-based cohort study. *Hepatology* **51**, 1675–1682 (2010).
13. Lauridsen, M. M. et al. In patients with cirrhosis, driving simulator performance is associated with real-life driving. *Clin. Gastroenterol. Hepatol.* **14**, 747–752 (2016).
14. Faccioli, J., Nardelli, S., Gioia, S., Riggio, O. & Ridola, L. Minimal hepatic encephalopathy affects daily life of cirrhotic patients: a viewpoint on clinical consequences and therapeutic opportunities. *J. Clin. Med.* **11**, 7246–7263 (2022).
15. San Martín-Valenzuela, C. et al. Motor and cognitive performance in patients with liver cirrhosis with minimal hepatic encephalopathy. *J. Clin. Med.* **9**, 2154–2169 (2020).
16. Seo, Y. S. & Shah, V. H. The role of gut-liver axis in the pathogenesis of liver cirrhosis and portal hypertension. *Clin. Mol. Hepatol.* **18**, 337–346 (2012).
17. Fukui, H. Gut-liver axis in liver cirrhosis: how to manage leaky gut and endotoxemia. *World J. Hepatol.* **7**, 425–442 (2015).
18. Qin, N. et al. Alterations of the human gut microbiome in liver cirrhosis. *Nature* **513**, 59–64 (2014).
19. Bajaj, J. S. et al. Altered profile of human gut microbiome is associated with cirrhosis and its complications. *J. Hepatol.* **60**, 940–947 (2014).
20. Chen, Y. et al. Characterization of fecal microbial communities in patients with liver cirrhosis. *Hepatology* **54**, 562–572 (2011).
21. Davis, B. C. & Bajaj, J. S. The human gut microbiome in liver diseases. *Semin. Liver Dis.* **37**, 128–140 (2017).
22. Tranah, T. H., Vijay, G. K., Ryan, J. M. & Shawcross, D. L. Systemic inflammation and ammonia in hepatic encephalopathy. *Metab. Brain Dis.* **28**, 1–5 (2013).
23. Sharma, B. C. et al. A randomized, double-blind, controlled trial comparing rifaximin plus lactulose with lactulose alone in treatment of overt hepatic encephalopathy. *Am. J. Gastroenterol.* **108**, 1458–1463 (2013).
24. Bass, N. M. et al. Rifaximin treatment in hepatic encephalopathy. *N. Engl. J. Med.* **362**, 1071–1081 (2010).
25. Ojetti, V. et al. Rifaximin pharmacology and clinical implications. *Expert Opin Drug Metab Toxicol*. **5**, 675–682 (2009).
26. Brown, E. L., Xue, Q., Jiang, Z. D., Xu, Y. & Dupont, H. L. Pretreatment of epithelial cells with rifaximin alters bacterial attachment and internalization profiles. *Antimicrob. Agents Chemother.* **54**, 388–396 (2010).
27. Schrodt, C., McHugh, E. E., Gawinowicz, M. A., Dupont, H. L. & Brown, E. L. Rifaximin-mediated changes to the epithelial cell proteome: 2-D gel analysis. *PLoS ONE* **8**, e68550 (2013).
28. Kang, D. J. et al. Rifaximin exerts beneficial effects independent of its ability to alter microbiota composition. *Clin. Transl. Gastroenterol.* **7**, e187 (2016).
29. Clarke, G. et al. Gut reactions: breaking down xenobiotic-microbiome interactions. *Pharmacol. Rev.* **71**, 198–224 (2019).
30. Sakaida, I. et al. Transplantation of bone marrow cells reduces CCl4-induced liver fibrosis in mice. *Hepatology* **40**, 1304–1311 (2004).
31. Derosa, L. et al. Intestinal *Akkermansia muciniphila* predicts clinical response to PD-1 blockade in patients with advanced non-small-cell lung cancer. *Nat. Med.* **28**, 315–324 (2022).
32. Karcher, N. et al. Genomic diversity and ecology of human-associated Akkermansia species in the gut microbiome revealed by extensive metagenomic assembly. *Genome Biol.* **22**, 209 (2021).
33. Depommier, C. et al. Pasteurized *Akkermansia muciniphila* increases whole-body energy expenditure and fecal energy excretion in diet-induced obese mice. *Gut Microbes* **11**, 1231–1245 (2020).

34. Plovier, H. et al. A purified membrane protein from Akkermansia muciniphila or the pasteurized bacterium improves metabolism in obese and diabetic mice. *Nat. Med.* **23**, 107–113 (2017).
35. Ratziu, V. A critical review of endpoints for non-cirrhotic NASH therapeutic trials. *J. Hepatol.* **68**, 353–361 (2018).
36. Liaw, Y. F. et al. Lamivudine for patients with chronic hepatitis B and advanced liver disease. *N. Engl. J. Med.* **351**, 1521–1531 (2004).
37. Ormerod, K. L. et al. Genomic characterization of the uncultured Bacteroidales family S24-7 inhabiting the guts of homeothermic animals. *Microbiome* **4**, 36 (2016).
38. Zagato, E. et al. Endogenous murine microbiota member Faecalibaculum rodentium and its human homologue protect from intestinal tumour growth. *Nat. Microbiol.* **5**, 511–524 (2020).
39. Cao, Y. G. et al. Faecalibaculum rodentium remodels retinoic acid signaling to govern eosinophil-dependent intestinal epithelial homeostasis. *Cell Host Microbe* **30**, 1295–1310.e1298 (2022).
40. Png, C. W. et al. Mucolytic bacteria with increased prevalence in IBD mucosa augment in vitro utilization of mucin by other bacteria. *Am. J. Gastroenterol.* **105**, 2420–2428 (2010).
41. de Vos, W. M. Microbe Profile: Akkermansia muciniphila: a conserved intestinal symbiont that acts as the gatekeeper of our mucosa. *Microbiology* **163**, 646–648 (2017).
42. Yang, J., Yang, H. & Li, Y. The triple interactions between gut microbiota, mycobiota and host immunity. *Crit. Rev. Food Sci. Nutr.* **63**, 11604–11624 (2023).
43. Schneeberger, M. et al. Akkermansia muciniphila inversely correlates with the onset of inflammation, altered adipose tissue metabolism and metabolic disorders during obesity in mice. *Sci. Rep.* **5**, 16643 (2015).
44. Everard, A. et al. Cross-talk between Akkermansia muciniphila and intestinal epithelium controls diet-induced obesity. *Proc. Natl Acad. Sci. USA* **110**, 9066–9071 (2013).
45. Hou, X. et al. Akkermansia Muciniphila potentiates the antitumor efficacy of FOLFOX in colon cancer. *Front. Pharmacol.* **12**, 725583 (2021).
46. Qu, S. et al. Akkermansia muciniphila alleviates dextran sulfate sodium (DSS)-induced acute colitis by NLRP3 activation. *Microbiol. Spectr.* **9**, e0073021 (2021).
47. Keshavarz Azizi Raftar, S. et al. The protective effects of live and pasteurized Akkermansia muciniphila and its extracellular vesicles against HFD/CCl4-induced liver injury. *Microbiol. Spectr.* **9**, e0048421 (2021).
48. Raftar, S. K. A. et al. The anti-inflammatory effects of Akkermansia muciniphila and its derivates in HFD/CCL4-induced murine model of liver injury. *Sci. Rep.* **12**, 2453 (2022).
49. Grander, C. et al. Recovery of ethanol-induced Akkermansia muciniphila depletion ameliorates alcoholic liver disease. *Gut* **67**, 891–901 (2018).
50. Suk, K. T. & Kim, D. J. Gut microbiota: novel therapeutic target for nonalcoholic fatty liver disease. *Expert Rev. Gastroenterol. Hepatol.* **13**, 193–204 (2019).
51. Im, E., Riegler, F. M., Pothoulakis, C. & Rhee, S. H. Elevated lipopolysaccharide in the colon evokes intestinal inflammation, aggravated in immune modulator-impaired mice. *Am. J. Physiol. Gastrointest. Liver Physiol.* **303**, G490–G497 (2012).
52. Hänninen, A. et al. Akkermansia muciniphila induces gut microbiota remodelling and controls islet autoimmunity in NOD mice. *Gut* **67**, 1445–1453 (2018).
53. Frazier, K. et al. High-fat diet disrupts REG3γ and gut microbial rhythms promoting metabolic dysfunction. *Cell Host Microbe* **30**, 809–823.e806 (2022).
54. Surana, N. K. & Kasper, D. L. Moving beyond microbiome-wide associations to causal microbe identification. *Nature* **552**, 244–247 (2017).
55. Bogatyrev, S. R., Rolando, J. C. & Ismagilov, R. F. Self-reinoculation with fecal flora changes microbiota density and composition leading to an altered bile-acid profile in the mouse small intestine. *Microbiome* **8**, 19 (2020).
56. Miyoshi, J. et al. Minimizing confounders and increasing data quality in murine models for studies of the gut microbiome. *PeerJ* **6**, e5166 (2018).
57. Reagan-Shaw, S., Nihal, M. & Ahmad, N. Dose translation from animal to human studies revisited. *FASEB J.* **22**, 659–661 (2008).
58. Miyoshi, J. et al. 5-aminosalicylic acid mediates expression of cyclooxygenase-2 and 15-hydroxyprostaglandin dehydrogenase to suppress colorectal tumorigenesis. *Anticancer Res.* **32**, 1193–1202 (2012).
59. Miyoshi, J. et al. Peripartum antibiotics promote gut dysbiosis, loss of immune tolerance, and inflammatory bowel disease in genetically prone offspring. *Cell Rep.* **20**, 491–504 (2017).
60. Bolyen, E. et al. Reproducible, interactive, scalable and extensible microbiome data science using QIIME 2. *Nat. Biotechnol.* **37**, 852–857 (2019).
61. Callahan, B. J. et al. DADA2: High-resolution sample inference from Illumina amplicon data. *Nat. Methods* **13**, 581–583 (2016).
62. Bushnell, B., Rood, J. & Singer, E. BBMerge - accurate paired shotgun read merging via overlap. *PLoS ONE* **12**, e0185056 (2017).
63. Bolger, A. M., Lohse, M. & Usadel, B. Trimmomatic: a flexible trimmer for Illumina sequence data. *Bioinformatics* **30**, 2114–2120 (2014).
64. Benson, G. Tandem repeats finder: a program to analyze DNA sequences. *Nucleic Acids Res.* **27**, 573–580 (1999).
65. Blanco-Míguez, A. et al. Extending and improving metagenomic taxonomic profiling with uncharacterized species using MetaPhlAn 4. *Nat. Biotechnol.* **41**, 1633–1644 (2023).
66. Mallick, H. et al. Multivariable association discovery in population-scale meta-omics studies. *PLoS Comput. Biol.* **17**, e1009442 (2021).

Acknowledgements

This work was supported by Grants-in-Aid for Scientific Research (KAKENHI: 20K08339 and 23K07360). We thank Edanz (https://jp.edanz.com/ac) for editing a draft of this manuscript. We also thank Eriko Nozaki (Core Laboratory for Proteomics and Genomics, Kyorin University School of Medicine) for her technical contribution to shotgun metagenomic sequencing.

Author contributions

N.O., J.M., M.M., and T.H. conceived the study, designed the experiments, and prepared the manuscript. N.O., J.M., Y.N., H.W., N.N., N.H., S.M., S.T.M.L., and T.O. performed the experiments and analyzed the data. N.K., M.M., and T.H. supervised the manuscript preparation. J.M. and T.H. oversaw the entire project. All authors have read and approved the manuscript.

Competing interests

J.M. has received grant support from AbbVie GK; and received consulting and lecture fees from EA Pharma Co., Ltd, AbbVie GK, Janssen Pharmaceutical K.K., Jansen Asia Pacific Pte. Ltd, Pfizer Inc., Mitsubishi Tanabe Pharma Corporation, JIMRO Co., Miyarisan Co., Ltd, and Takeda Pharmaceutical Co., Ltd. M.M. has received consulting and lecture fees from Janssen Pharmaceutical K.K., Takeda Pharmaceutical Co., Ltd, AbbVie GK, Mitsubishi Tanabe Pharma Corporation, Kyorin Pharmaceutical Co., Ltd, Mochida Pharmaceutical Co., Ltd, JIMRO Co., Nippon Kayaku Co., Ltd, Mylan EPD G.K., and Aspen Japan Co., Ltd. T.H. has performed Joint Research with Alfresa Pharma Co., Ltd, and EA Pharma Co., Ltd; received grant support from AbbVie GK, Boston Scientific Corp., EA Pharma Co., Ltd, JIMRO Co., Ltd, Mitsubishi Tanabe Pharma Corporation, Mochida Pharmaceutical Co., Ltd, Nippon Kayaku Co., Ltd, Pfizer Inc., and Takeda Pharmaceutical Co., Ltd, and received consulting and lecture fees from AbbVie GK, EA Pharma Co., Ltd, Janssen Research & Development, LLC., Gilead Sciences Inc., Eli Lilly and Co., Bristol Myers Squibb, Mitsubishi Tanabe Pharma Corporation, Takeda Pharmaceutical Co., Ltd, Mochida

Pharmaceutical Co., Ltd, and Kissei Pharmaceutical Co., Ltd. All other authors declare no financial or non-financial competing interests.

Additional information

Supplementary information The online version contains supplementary material available at https://doi.org/10.1038/s41522-024-00564-y.

Correspondence and requests for materials should be addressed to Jun Miyoshi or Tadakazu Hisamatsu.